that the uptake had reached its maximum at 2 hours.
11. Oocytes were incubated in 0.5 μM [^{3}H]glutamine overnight at 19°C. In experiments where ACh secretion from oocytes injected with *Torpedo* mRNA was assayed, 1 μM [^{14}C]acetate was used in the overnight incubation. After three washes in Ca^{2+}- and Mg^{2+}-free ORII medium [82.5 mM NaCl, 2.5 mM KCl, 5 mM Hepes (pH 7.5)], groups of five oocytes were transferred to wells containing 0.5 ml of ORII medium supplemented with 10 mM, 5 mM, or 0 mM Ca^{2+} in the presence or absence of 10 μM A23187 Ca^{2+} ionophore (Calbiochem, La Jolla, CA) (final dimethyl sulfoxide concentration 0.1%). After 10 min, the oocytes were transferred to a well containing 1 ml of Ca^{2+}- and Mg^{2+}-free ORII to stop the release of transmitter. The two supernatants were combined in a scintillation vial with 15 ml of scintillation fluid and the radioactivity was counted. We have tried high concentrations of extracellular K^+ (50 mM) to depolarize the oocyte membrane and found no depolarization-dependent release of glutamate. Veratridine does cause release, although to a lesser extent than the Ca^{2+} ionophore. The failure of the oocyte to respond to depolarization was likely due to a deficiency in the expression of voltage-dependent Ca^{2+} channels in these oocytes.
12. E. M. Adler *et al.*, *J. Neurosci.* **11**, 1496 (1991). For experiments involving BAPTA-AM, oocytes were preincubated for 15 min with Ca^{2+}-free ORII containing 1 mM BAPTA, and 1 mM BAPTA was present during the ionophore application. The basal level of release from water-injected oocytes was not affected by BAPTA treatment.
13. F. Valtorta *et al.*, *J. Cell Biol.* **107**, 2717 (1988).
14. F. Valtorta, unpublished observations.
15. *Xenopus* oocytes were fixed for 2 hours at room temperature in 2% formaldehyde plus 0.2% glutaraldehyde plus 100 mM sodium phosphate buffer (pH 7.0). Small wedges of oocytes were dissected, washed for 1 hour in 100 mM sodium phosphate buffer (pH 7.0), infiltrated in 2.3 M sucrose, and frozen in Freon 22 cooled with liquid nitrogen. Ultrathin frozen sections were prepared with an Ultracut microtome equipped with an FC4 attachment (Reichert Jung, Austria), were collected onto Formvar-coated nickel grids, and were processed for immunogold labeling as described [F. Torri-Tarelli *et al.*, *J. Cell Biol.* **110**, 449 (1990)]. Rabbit antisera against frog synaptophysin and immunoglobulin G, fractions were prepared as described (*13*).
16. P. De Camilli *et al.*, *EMBO J.* **10**, 1275 (1991).
17. R. E. Leube, B. Weidenmann, W. W. Franke, *Cell* **59**, 433 (1989); P. A. Johnston *et al.*, *EMBO J.* **8**, 2863 (1989); A. D. Linstedt and R. B. Kelly, *Neuron* **7**, 309 (1991).
18. R. E. Leube *et al.*, *EMBO J.* **6**, 3261 (1987); K. M. Buckley, E. Floor, R. B. Kelly, *J. Cell Biol.* **105**, 2447 (1987); T. C. Südhof *et al.*, *Science* **238**, 1142 (1987).
19. P. A. Johnson, R. Jahn, T. C. Südhof, *J. Biol. Chem.* **264**, 1258 (1989); P. Knaus and H. Betz, *FEBS Lett.* **261**, 358 (1990).
20. C. Cazenave *et al.*, *Nucleic Acids Res.* **15**, 10507 (1987); P. Dash *et al.*, *Proc. Natl. Acad. Sci. U.S.A.* **84**, 7896 (1987); J. Shuttleworth *et al.*, *Gene* **72**, 267 (1988).
21. Oligonucleotides were prepared on a Pharmacia DNA synthesizer and deprotected in ammonium hydroxide, which was then evaporated in a Speed-Vac. The oligonucleotides were desalted by reprecipitation with NaCl and ethyl alcohol in the presence of glycogen. Sense rat cerebellar synaptophysin oligonucleotide: ATGGACGTGGTGAATCAGC. Antisense rat synaptophysin oligonucleotide: GCTGATTCACCACGTCCAT. Antisense *Torpedo* synaptophysin oligonucleotide: TCTGGTTGACGATCTCCAT [D. Cowan, M. Linial, R. H. Scheller, *Brain Res.* **509**, 1 (1990)]. The rat sense oligonucleotides were also used in the *Torpedo* experiments as a control.
22. Oocytes were sonicated in homogenization buffer [20 mM tris (pH 7.6), 50 mM NaCl, 1% Triton X-100, 1 mM phenylmethylsulfonyl fluoride, 1 mM iodoacetamide, aprotinin (200 U/ml)]. The homogenates were subjected to low-speed centrifugation (10,000*g*, 15 min) to separate yolk granules. Total protein from one oocyte was loaded onto each lane, was separated by SDS-PAGE electrophoresis, and was blotted onto nitrocellulose membrane. The blot was incubated with a monoclonal antibody specific to rat synaptophysin or an antiserum to synaptobrevin followed by ^{125}I-labeled protein A and autoradiography.
23. M. Baumert *et al.*, *EMBO J.* **8**, 379 (1989).
24. This frog polyclonal anti-synaptophysin antibody is known to have diverse cross-reactivity, including goldfish and rat (F. Valtorta, unpublished observations).
25. D. G. Nicholls, T. S. Sihra, J. Sanchez-Prieto, *J. Neurochem.* **49**, 50 (1987); D. G. Nicholls and T. S. Sihra, *Nature* **321**, 772 (1986). Oocytes were placed in a cuvette with 2 ml of ORII solution either with 10 mM or 0 mM $[Ca^{2+}]_o$. $NADP^+$ (1 mM) and 50 units of L-glutamate dehydrogenase were added and, after the initial exogenous glutamate was assayed, 10 μM Ca^{2+} ionophore (ionomycin) was added. Ionomycin was used instead of A23187 because the intrinsic fluorescence of the latter interfered with the assay. A Perkin-Elmer spectrofluorimeter (U 50) and a fluorescence data manager program with excitation at 330 nm and emission at 460 nm were used to monitor the increase of fluorescence over time. For final glutamate release values, oocytes were stimulated with the ionophore in a small petri dish, the supernatant (2 ml) was transferred to a cuvette where $NADP^+$ and glutamate dehydrogenase were added, and the fluorescence was measured. Total glutamate content was determined after solubilization of the oocytes in 0.4% Triton X-100.
26. H. Rehm, B. Wiedenmann, H. Betz, *EMBO J.* **5**, 535 (1986).
27. P. A. Johnston and T. C. Südhof, *J. Biol. Chem.* **264**, 7849 (1990).
28. L. Thomas and H. Betz, *J. Cell Biol.* 11, 2041 (1990); T. C. Südhof and R. Jahn, *Neuron* **6**, 665 (1991).
29. L. Thomas *et al.*, *Science* **292**, 1050 (1988).
30. This work was supported by grants from USPHS to M-m.P. (NS 22764) and to P.G. (MH 39327), and from NSF to M-m.P. (BNS 13306 and BNS 12398). J.A. was supported by a NSF Predoctoral Fellowship. We thank A. Cavelli, Y. Dunant, D. Weilner, R. Blakely, and S. Omara for valuable communications; N. Iezzi for performing the electron microscopy experiments; and R. Jahn and J. Rubenstein for the gift of antibodies.

13 April 1992; accepted 16 June 1992

Functional Modulation of $GABA_A$ Receptors by cAMP-Dependent Protein Phosphorylation

Stephen J. Moss, Trevor G. Smart, Craig D. Blackstone, Richard L. Huganir*

γ-Aminobutyric $acid_A$ ($GABA_A$) receptors are ligand-gated ion channels that mediate inhibitory synaptic transmission in the central nervous system. The role of protein phosphorylation in the modulation of $GABA_A$ receptor function was examined with cells transiently transfected with $GABA_A$ receptor subunits. $GABA_A$ receptors consisting of the α_1 and β_1 or the α_1, β_1, and γ_2 subunits were directly phosphorylated on the β_1 subunit by adenosine 3′,5′-monophosphate (cAMP)–dependent protein kinase (PKA). The phosphorylation decreased the amplitude of the GABA response of both receptor types and the extent of rapid desensitization of the $GABA_A$ receptor that consisted of the α_1 and β_1 subunits. Site-specific mutagenesis of the serine residue phosphorylated by PKA completely eliminated the PKA phosphorylation and modulation of the $GABA_A$ receptor. In primary embryonic rat neuronal cell cultures, a similar regulation of $GABA_A$ receptors by PKA was observed. These results demonstrate that the $GABA_A$ receptor is directly modulated by protein phosphorylation and suggest that neurotransmitters or neuropeptides that regulate intracellular cAMP levels may modulate the responses of neurons to GABA and consequently have profound effects on synaptic excitability.

Molecular cloning of $GABA_A$ receptor subunits has revealed a large number of diverse subunits that can be divided into five classes—α, β, γ, δ, and ρ—on the basis of sequence similarity (*1–4*). Expression of different combinations of these subunits in heterologous systems produces $GABA_A$ receptors that vary in their pharmacology and ion channel properties (*1*). The major intracellular domains of many of these receptor subunits contain consensus sites for protein phosphorylation by PKA, protein kinase C, and protein tyrosine kinases (*5*).

To examine directly the phosphorylation of $GABA_A$ receptors, we expressed the α_1 and β_1 or the α_1, β_1, and γ_2 subunits in human embryonic kidney 293 (HEK293) cells (*6–9*). These cells were labeled with [^{35}S]methionine, and the $GABA_A$ receptors were isolated by immunoprecipitation with antibodies to a bacterial fusion protein containing the major intracellular domain of the β_1 subunit (anti-β_1) (Fig. 1A) (*9*). The α_1 subunit migrated as a 52-kD protein, whereas the β_1 subunit migrated as a 58-kD protein with a proteolytic break-

S. J. Moss, C. D. Blackstone, R. L. Huganir, Department of Neuroscience, Howard Hughes Medical Institute, The Johns Hopkins University School of Medicine, Baltimore, MD 21205.
T. G. Smart, The School of Pharmacy, Department of Pharmacology, London, United Kingdom WCIN 1AX.
*To whom correspondence should be addressed.

down product of 56 kD (Fig. 1A) (9). The γ_2 subunit was difficult to detect biochemically and appeared to be sensitive to proteolysis, migrating as a diffuse band at approximately 42 kD (*10*). When transfected HEK293 cells were labeled with [^{32}P]orthophosphate, subsequent immunoprecipitation of the $GABA_A$ receptor demonstrated that the β_1 subunit has a small amount of basal phosphorylation (Fig. 1B) (9). No basal phosphorylation of the α_1 and γ_2 subunits was detected (*10*).

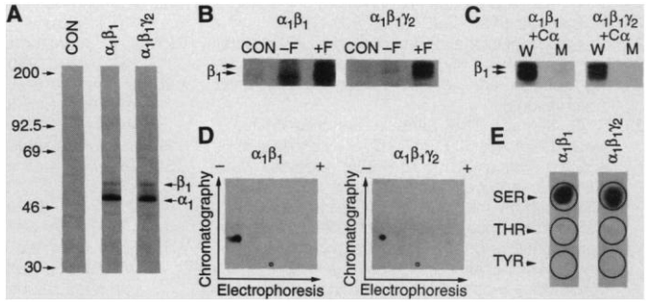

Fig. 1. Phosphorylation of the β_1 subunit of recombinant murine $GABA_A$ receptors by PKA. HEK293 cells transiently expressing the α_1 and β_1 subunits ($\alpha\beta$) or the α_1, β_1, and γ_2 subunits ($\alpha\beta\gamma$) were labeled with (**A**) [^{35}S]methionine or with (**B**) [^{32}P]orthophosphate. In (A), the expressed $GABA_A$ receptors were solubilized from the cell membranes and immunoprecipitated with anti-β_1 antibodies. The immune complexes were then resolved by SDS-PAGE and analyzed by autoradiography. CON indicates immunoprecipitations from mock-transfected cells. Molecular size markers are indicated to the left in kilodaltons. In (B), membranes from mock-transfected (CON) and transfected cells treated with (+F) or without (−F) forskolin (20 μM) for 30 min were solubilized, and the recombinant $GABA_A$ receptors were immunoprecipitated and analyzed as in (A). (**C**) The HEK293 cells transiently transfected with the $\alpha\beta$ or $\alpha\beta\gamma$ subunits with either the wild-type (W) or mutant (M) form of the β_1 subunit were cotransfected with Cα cDNA (*12*), which encodes the catalytic subunit of PKA. The cells were labeled with [^{32}P]orthophosphate, and the $GABA_A$ receptors were then immunoprecipitated and analyzed as in (A). In the mutant β_1 subunit (M), Ser^{409} was converted to an alanine (S409A) residue by site-specific mutagenesis to eliminate the site for phosphorylation by PKA. (**D**) The phosphorylated β_1 subunits isolated from cells in (C) were analyzed by phosphopeptide mapping. Gel slices that contained both forms of the β_1 subunit were excised and digested with trypsin. The resulting phosphopeptides were then subjected to two-dimensional phosphopeptide mapping and visualized by autoradiography. Identical results were obtained upon peptide map analysis of the isolated β_1 subunit when phosphorylated after activation of the endogenous PKA. (**E**) The phosphoamino acid content of the phosphorylated β_1 subunit was determined. The phosphopeptide shown in (C) was subjected to acid hydrolysis, and the phosphoamino acids were separated by electrophoresis. The positions of the phosphoserine, phosphothreonine, and phosphotyrosine standards are indicated. Phosphorylation of the β_1 subunit by the endogenous PKA also occurred exclusively on serine residues.

Treatment of the cells that expressed either the α_1 and β_1 or the α_1, β_1, and γ_2 subunits with the adenylate cyclase activator forskolin increased the phosphorylation of the β_1 subunit (Fig. 1B). Forskolin had no effect on phosphorylation of the α_1 and γ_2 subunits (*10*). Co-expression of a cDNA encoding the catalytic subunit of PKA (*11*) (Cα) with the α_1 and β_1 or the α_1, β_1, and γ_2 subunits resulted in constitutive phosphorylation of the receptor on only the β_1 subunit (Fig. 1C). The phosphorylation of the β_1 subunit in both cases occurred exclusively on serine residues within a single phosphopeptide, as determined by phosphoamino acid analysis and two-dimensional phosphopeptide mapping of tryptic digests of the isolated β_1 subunit (Fig. 1, D and E). These phosphopeptide maps were identical to phosphopeptide maps of a β_1 subunit fusion protein phosphorylated by the purified catalytic subunit of PKA (*12*). All $GABA_A$ receptor β subunits isolated to date have a consensus site for adenosine 3′,5′-monophosphate (cAMP)–dependent phosphorylation in the major intracellular loop between the third and fourth putative transmembrane domains (*5*). Mutation of this serine residue (Ser^{409}) to an alanine residue by site-specific mutagenesis eliminated the phosphorylation of the β_1 subunit by the endogenous PKA (*10*) and by the cotransfected catalytic subunit of PKA (Fig. 1C). These results identify Ser^{409} as the site phosphorylated by PKA and provide additional evidence that the 58-kD and 56-kD proteins are different forms of the β_1 subunit.

To examine the functional effects of β_1

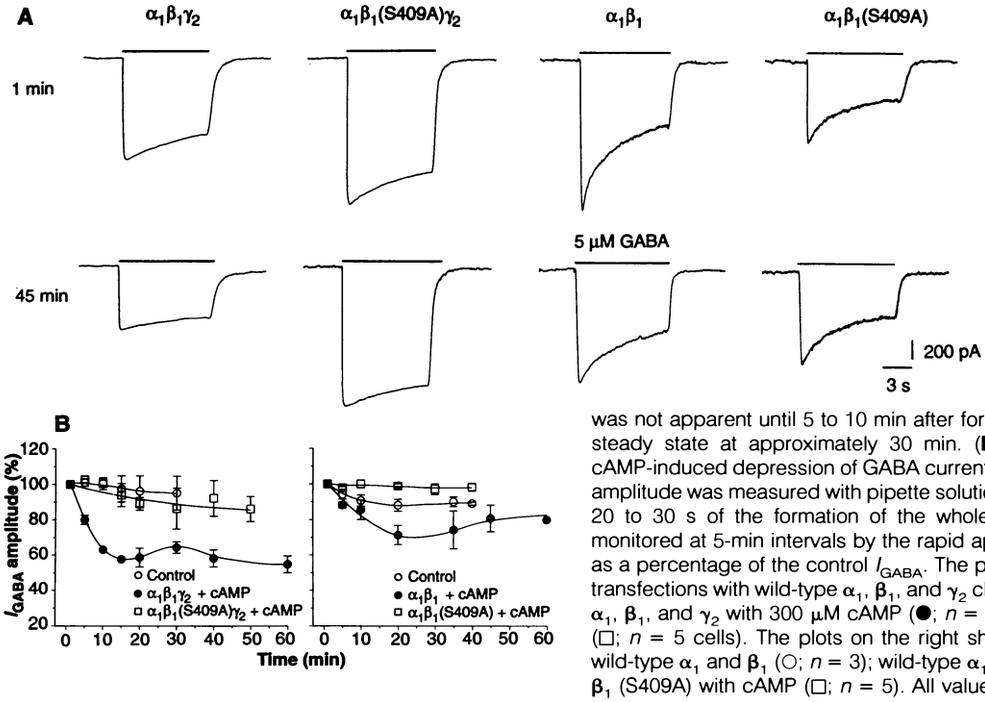

Fig. 2. Effect of intracellular cAMP on GABA-induced membrane currents in transfected HEK293 cells. (**A**) Membrane currents evoked by the rapid application of GABA (5 μM) were recorded under voltage clamp at a holding potential of −50 mV in cells transiently expressing the α_1, β_1, and γ_2 subunits or the α_1 and β_1 subunits with either the wild-type β_1 subunit or a mutant β_1 (S409A) subunit. The $GABA_A$-induced currents were recorded 1 min (top row) and 45 min (bottom row) after formation of the whole-cell recording mode. The cAMP (300 μM) was included in the patch pipette recording solution. The effect of intracellular perfusion of cAMP was not apparent until 5 to 10 min after formation of the whole-cell patch, reaching a steady state at approximately 30 min. (**B**) Analysis of the time dependence for cAMP-induced depression of GABA current (I_{GABA}) in HEK293 cells. The control I_{GABA} amplitude was measured with pipette solutions with and without cAMP (300 μM) within 20 to 30 s of the formation of the whole-cell configuration. GABA currents were monitored at 5-min intervals by the rapid application of GABA (5 μM) and expressed as a percentage of the control I_{GABA}. The plots on the left present data from separate transfections with wild-type α_1, β_1, and γ_2 cDNAs for control cells (○; n = 4); wild-type α_1, β_1, and γ_2 with 300 μM cAMP (●; n = 3); and α_1, β_1 (S409A), and γ_2 with cAMP (□; n = 5 cells). The plots on the right show data from separate transfections with wild-type α_1 and β_1 (○; n = 3); wild-type α_1 and β_1 with cAMP (●; n = 3); and α_1 and β_1 (S409A) with cAMP (□; n = 5). All values are presented as means ± SEM.

Table 1. Analysis of the decay of GABA-induced currents. GABA currents were recorded from HEK293 cells and from neurons under whole-cell voltage clamp. Values (in seconds) represent means ± SD from 3 to 12 cells; the percentage contribution of the time constant to the overall decay is indicated in parentheses. All values were determined after the rapid application of 5 μM GABA to cells recorded with a normal pipette solution (Fig. 2) or with a pipette solution that contained either cAMP (300 μM) or PKA (47 μg/ml). Decay time constants were also determined from cells cotransfected with the cDNAs for the GABA receptor subunits and Cα. Dashes represent conditions not examined.

Treatment	Receptors				
	$\alpha_1\beta_1$	$\alpha_1\beta_1$(S409A)	$\alpha_1\beta_1\gamma_2$	$\alpha_1\beta_1$(S409A)γ_2	Neuronal GABA receptor
Control	1.62 ± 0.09 (67) 30.32 ± 7.65 (33)	2.05 ± 0.04 (47) 39.03 ± 13.3 (53)	32.05 ± 3.24 (100)	40.67 ± 7.42 (100)	1.08 ± 0.06 (69) 17.71 ± 3.42 (31)
cAMP	1.33 ± 0.25 (21) 23.88 ± 3.51 (79)	1.66 ± 0.5 (40) 37.09 ± 12.9 (60)	—	—	—
PKA	—	—	38.06 ± 4.65 (100)	—	1.43 ± 0.11 (40) 20.45 ± 5.21 (60)
Cα	1.64 ± 0.24 (14) 35.65 ± 10.33 (86)	1.95 ± 0.39 (41) 42.25 ± 9.18 (59)	38.31 ± 7.23 (100)	50.91 ± 6.46 (100)	—

subunit phosphorylation, we used whole-cell patch-clamp techniques to study both recombinant and native neuronal $GABA_A$ receptors (*13*). The $GABA_A$ receptor that consisted of the α_1, β_1, and γ_2 subunits desensitized slowly upon the application of GABA, whereas the $\alpha_1\beta_1$ receptor desensitized much more rapidly (*14*) (Fig. 2A). Although decline in the GABA-induced current was usually best fit by a single exponential decay for $\alpha_1\beta_1\gamma_2$ receptors, a double exponential function was usually necessary to describe the current decay for the $\alpha_1\beta_1$ receptors (Fig. 3B). The response to GABA mediated by the receptors consisting of the α_1, β_1, and γ_2 subunits was relatively insensitive to Zn^{2+} but potentiated by benzodiazepines (*10, 15*), whereas receptors composed of α_1 and β_1 subunits were inhibited by Zn^{2+} and were insensitive to benzodiazepines (*10, 14–16*).

When HEK293 cells that expressed the α_1, β_1, and γ_2 or the α_1 and β_1 subunits were intracellularly perfused with cAMP (*13*), the peak amplitudes of the GABA-induced currents decreased (Fig. 2). The inhibition of the peak responses by cAMP was apparent within 5 to 10 min after the whole-cell patch was formed and reached a steady state after 20 to 30 min. (Fig. 2, A and B). The effect of cAMP on the response to GABA was greater with $GABA_A$ receptors composed of α_1, β_1, and γ_2 subunits but was also apparent with receptors that consisted of the α_1 and β_1 subunits. Site-specific mutagenesis of Ser^{409} phosphorylated by PKA to an alanine residue completely eliminated the modulation of the GABA responses by cAMP (Fig. 2, A and B). In addition to the cAMP-induced decrease in the amplitude of GABA responses, the fast component of desensitization was reduced for $GABA_A$ receptors that consisted of the α_1 and β_1 subunits, although the rates of desensitization were unaltered (Fig. 2) (Table 1). Site-specific mutagenesis of the phosphorylation site also completely eliminated modulation by cAMP of the desensitization kinetics of the $\alpha_1\beta_1$ receptor (Fig. 2) (Table 1).

To examine the effect of cAMP on the desensitization kinetics in more detail, we co-expressed the α_1 and β_1 subunits with the catalytic subunit of PKA (Cα) to produce a constitutively phosphorylated $GABA_A$ receptor. These $GABA_A$ receptors exhibited desensitization kinetics identical to those seen in the cAMP-treated cells (Fig. 3) (Table 1). This apparent slowing of the desensitization rate was mostly a result of a decrease in the proportion of the fast component of desensitization; PKA phosphorylation apparently had little effect on the time constants of the rapid and slow phases of desensitization (Table 1) (Fig. 3B). Mutation of Ser^{409} caused the desensitization kinetics of the receptors cotransfected with the catalytic subunit of PKA to revert to those of non-phosphorylated wild-type $GABA_A$ receptors (Fig. 3). In contrast to the desensitization kinetics of receptors composed of α_1

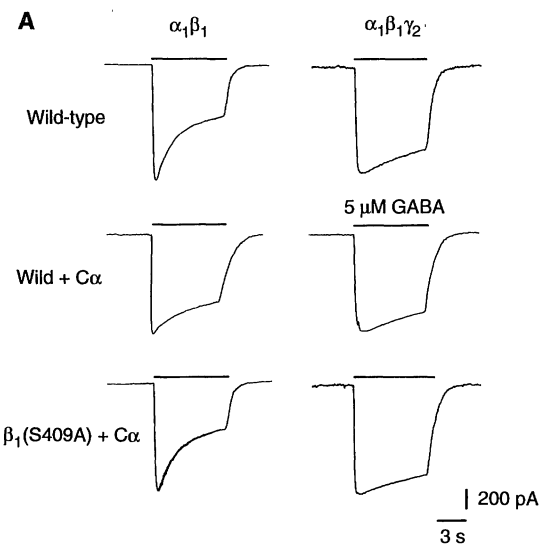

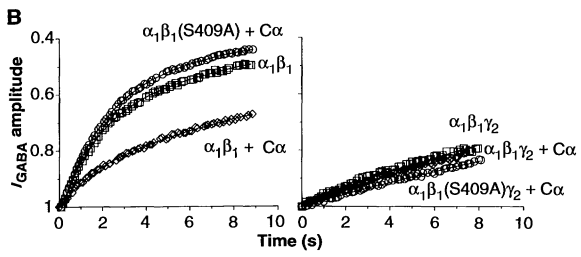

Fig. 3. Phosphorylation of the $GABA_A$ receptor affects desensitization in receptors composed of α_1 and β_1 subunits. (**A**) Whole-cell recordings of GABA-induced membrane currents after rapid application of GABA (5 μM) to transiently transfected HEK293 cells under voltage clamp. Six different cells were used after transfection with the following cDNA combinations: $\alpha_1\beta_1$ and $\alpha_1\beta_1\gamma_2$ wild-type cDNAs (top row); $\alpha_1\beta_1$ and $\alpha_1\beta_1\gamma_2$ cotransfected with the Cα plasmid (middle row); cotransfection of Cα with $GABA_A$ receptors containing a mutated β_1 subunit cDNA, $\alpha_1\beta_1$ (S409A), or $\alpha_1\beta_1$ (S409A)γ_2 (bottom row). Holding potential was −50 mV. (**B**) Decay curves for the GABA-induced currents are plotted from the records shown in (A) and are fitted with a mono- or biexponential decay with a Marquardt nonlinear least squares fitting routine. GABA-evoked current decays were normalized to the peak current induced in each cell. Cells expressing $GABA_A$ receptors with only the α_1 and β_1 subunits (plots on left) displayed biexponentially decaying currents with fast (τ_f) and slow (τ_s) time constants; $\alpha_1\beta_1$ (□), τ_f = 1.85 ± 0.04 s (40%) and τ_s = 35.63 ± 1.66 s (60%); $\alpha_1\beta_1$ + Cα (◇), τ_f = 1.24 ± 0.06 s (17%) and τ_s = 22.91 ± 0.36 s (83%); $\alpha_1\beta_1$ (S409A) + Cα (○), τ_f = 2.05 ± 0.04 s (47%) and τ_s = 30.03 ± 2.51 (53%). $GABA_A$ receptors containing the γ_2 subunit (plots on right) exhibited declining currents generally approximated by monoexponential decays with the following time constants: $\alpha_1\beta_1\gamma_2$ (□), 34.53 ± 1.65 s; $\alpha_1\beta_1\gamma_2$ + Cα (◇), 36.78 ± 0.24 s; and $\alpha_1\beta_1$(S409A)γ_2 + Cα (○), 45.91 ± 0.27 s. Amplitude of I_{GABA} is normalized to the peak currents.

and β_1 subunits, the desensitization kinetics of the receptors consisting of the α_1, β_1, and γ_2 subunits were only slightly affected by PKA phosphorylation (Fig. 3).

These results demonstrate that phosphorylation of $GABA_A$ receptors on Ser^{409} of the β_1 subunit decreases the peak amplitude of their response to GABA. In addition, phosphorylation slows the apparent rate of desensitization of receptors consisting of the α_1 and β_1 subunits by decreasing the proportion of the fast component of desensitization. To examine whether this modulation also occurs in neurons, we studied $GABA_A$ receptors in rat embryonic (day E21) primary neuronal cultures prepared from superior cervical ganglia (*13*). $GABA_A$ receptors in these cultures are sensitive to inhibition by Zn^{2+}, and their function is potentiated by benzodiazepines, which suggests that they may be heterogeneous and consist of both $\alpha\beta$ and $\alpha\beta\gamma$ receptors (*15–17*). The large degree of inhibition caused by Zn^{2+} in embryonic neurons (*16*) and the biexponential decay of the GABA-induced current (Fig. 4B) suggested that $GABA_A$ receptors composed of α and β subunits comprise the most abundant receptor population in these cells at this stage of development (*14–17*).

GABA-induced currents in these neurons desensitized rapidly but exhibited virtually no changes in GABA responses over several hours of recording (Fig. 4A). Repatching the same neurons with a patch electrode that contained purified PKA in the pipette solution decreased the peak amplitude of the GABA response and the fast component of receptor desensitization (Fig. 4A). This effect was apparent within 5 min and reached a steady state after approximately 30 min. Repatching the same neuron for a third time with a pipette solution that contained a peptide inhibitor of PKA (PKI; 400 μg/ml) produced a partial recovery of the peak amplitude and of the fast component of receptor desensitization (Fig. 4). Thus, intracellular perfusion of neurons with PKA produces functional effects on the native $GABA_A$ receptors that are apparently identical to those seen upon PKA phosphorylation of recombinant $GABA_A$ receptors in transfected cells.

Many studies have suggested that $GABA_A$ receptors are regulated by protein phosphorylation; however, the results have been complex and sometimes contradictory (*5*, *18*). Purified preparations of the $GABA_A$ receptor can be phosphorylated in vitro by PKA and protein kinase C (*19*, *20*). Physiological studies have suggested that phosphorylation of $GABA_A$ receptors by various protein kinases inhibits (*21–23*), potentiates (*24*), or has no effect (*25*) on $GABA_A$ receptor function. Our results demonstrate that the peak response and desensitization kinetics of $GABA_A$ receptors are modulated by cAMP-dependent phosphorylation of the β_1 subunit. The apparent contradictory effects of phosphorylation of $GABA_A$ receptors reported in previous studies may be a result of different functional effects of phosphorylation of β subunit subtypes or the subunit composition of the receptors being studied. Protein phosphorylation of the nicotinic acetylcholine receptor increases the rate of the rapid phase of desensitization (*5*, *26*), which suggests that desensitization of ligand-gated ion channels may be a common property of these receptors that is regulated by protein phosphorylation (*5*).

Finally, our results suggest that, in general, protein phosphorylation may mediate receptor-to-receptor interactions between G protein–linked receptors and ligand-gated ion channels at many synapses in the central nervous system. Neurotransmitters and neuropeptides that regulate intracellular second messengers, such as cAMP, may modulate the responses of ligand-gated ion channels in the postsynaptic membrane and thus may have profound effects on synaptic excitability.

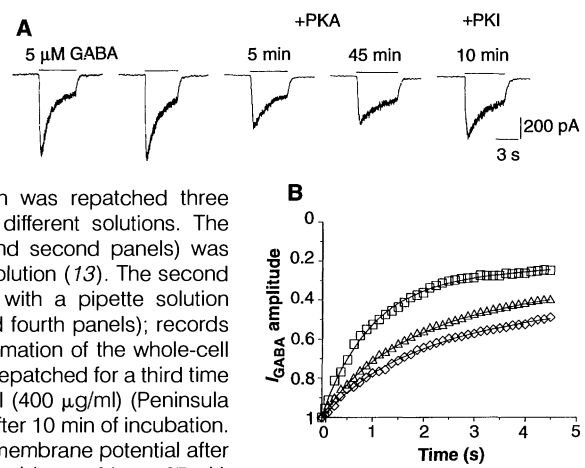

Fig. 4. Effect of PKA on GABA-induced currents in cultured sympathetic ganglion neurons. (**A**) Whole-cell voltage-clamp recordings illustrating the effect of rapid superfusion of 5 μM GABA resulting in reproducible currents with biphasic decays. The same neuron was repatched three times with pipettes that contained different solutions. The control whole-cell recording (first and second panels) was obtained with the standard pipette solution (*13*). The second whole-cell recording was obtained with a pipette solution containing PKA (47 μg/ml) (third and fourth panels); records were taken at 5 and 45 min after formation of the whole-cell recording mode. The same cell was repatched for a third time with a pipette solution containing PKI (400 μg/ml) (Peninsula Labs); the fifth panel was recorded after 10 min of incubation. Holding potential was −55 mV. The membrane potential after the formation of each whole cell was stable at −61 to −67 mV. (**B**) Decays of the GABA-induced currents were fitted with two component exponential functions. The fast (τ_f) and slow (τ_s) time constants and their relative percent contribution to the overall decay are: normal pipette solution (□), τ_f = 0.92 ± 0.06 s (67%) and τ_s = 17.4 ± 8.65 s (33%); + PKA pipette solution (◇), τ_f = 1.52 ± 0.25 s (38%) and τ_s = 19.36 ± 7.21 s (62%); and + PKI pipette solution (△), τ_f = 1.29 ± 0.09 s (48%) and τ_s = 12.45 ± 1.72 s (52%). Amplitude of I_{GABA} is normalized to the peak currents.

REFERENCES AND NOTES

1. D. R. Burt and G. L. Komatchi, *FASEB J.* **5**, 2916 (1991).
2. P. R. Schofield *et al.*, *Nature* **328**, 221 (1987).
3. E. S. Levitan *et al.*, *ibid.* **335**, 76 (1988).
4. R. W. Olsen and A. J. Tobin, *FASEB J.* **4**, 1469 (1990).
5. S. L. Swope, S. J. Moss, C. D. Blackstone, R. L. Huganir, *ibid.* **6**, 2514 (1992).
6. D. B. Pritchett *et al.*, *Science* **242**, 1306 (1988).
7. D. B. Pritchett *et al.*, *Nature* **338**, 582 (1989).
8. S. J. Moss *et al.*, *Neurosci. Lett.* **123**, 265 (1991).
9. The cDNA clone encoding the γ_2 (γ_2S) subunit of the murine $GABA_A$ receptor has been described (*27*). The murine α_1 and β_1 subunits (*28*) were isolated by low-stringency screening of a murine cDNA library with bovine $GABA_A$ receptor cDNA probes (*2*). These cDNAs were subcloned as Eco RI fragments into the mammalian expression vector pGW1 (*8*). Expression of cloned DNA in this vector is driven by the cytomegalovirus promoter. Site-directed mutagenesis of the β_1 subunit cDNA was performed as described (*29*) with the oligonucleotide 5′-GAGCTGCGGGGCGCGCC-3′ to convert Ser^{409} into an alanine residue. The fidelity of this substitution in the final expression plasmid was confirmed by DNA sequence analysis. The cDNA for the murine PKA catalytic subunit (Cα) (*11*) was also subcloned into pGW1. HEK293 cells (American Type Culture Collection CRL 1573) were transfected by calcium phosphate coprecipitation (*8*) with CsCl-purified DNA (20 μg per 10-cm plate). $GABA_A$ receptor cDNAs were transfected in equimolar ratios; the Cα plasmid (3 μg of DNA per plate) was included where indicated. Forty-eight hours after transfection, the cells were metabolically labeled with [^{35}S]methionine (1 mCi/ml; trans [^{35}S-]label, ICN Pharmaceuticals) for 3 hours in methionine-free media or with [^{32}P]orthophosphate (2 mCi/ml; DuPont Biotechnology Systems) for 4 hours in phosphate-free medium. After metabolic labeling, the cells were lysed by sonication in buffer [20 mM sodium phosphate (pH 7.0), 50 mM NaF, 1 mM sodium orthovanadate, 10 mM sodium pyrophosphate, 150 mM NaCl, 5 mM EDTA, 5 mM EGTA, 1 mM phenylmethylsulfonyl fluoride, 1 mM benzamidine, leupeptin (10 μg/ml), antipain (10 μg/ml), pepstatin (10 μg/ml), Trasylol (aprotinin) (10 U/ml), bovine serum albumin (0.1%), Triton X-100 (2.0%), and deoxycholate (0.5%)]. The $GABA_A$ receptor complexes were immunoprecipitated with a rabbit polyclonal antiserum to a fusion protein of the major intracellular domain of the β_1 subunit (*12*) (anti-β_1) coupled to protein A–Sepharose CL-4B (Pharmicia). Receptor complexes were then resolved by SDS–polyacrylamide gel electrophoresis (SDS-PAGE) (8% gels). The 52-kD protein was identified as the α_1 subunit because this protein was also immunoprecipitated by an antiserum specific for a peptide from the α_1 subunit under denaturing conditions; immunoprecipitation was completely blocked by preadsorption of the antibodies with the peptide (*10*). The 56- and 58-kD polypeptides were identified as β_1 subunits because they could be specifically immunoprecipitated under denaturing conditions with anti-β_1 antibodies. Furthermore, this immunoprecipitation was abolished by preadsorption of the antiserum with an excess of the fusion protein. The two-dimensional tryptic phosphopeptide

maps and the phosphoamino acid analysis were done as described (*30*).
10. S. J. Moss, T. G. Smart, C. D. Blackstone, R. L. Huganir, unpublished observations.
11. M. D. Uhler *et al.*, *Proc. Natl. Acad. Sci. U.S.A.* **83**, 1300 (1986).
12. S. J. Moss, C. A. Doherty, R. L. Huganir, *J. Biol. Chem.* **267**, 14470 (1992).
13. The HEK293 cells were maintained as described (*8*, *15*). Recordings were made at 25°C from cells superfused with a Krebs solution containing 5 mM Hepes (pH 7.4), 140 mM NaCl, 4.7 mM KCl, 1.2 mM $MgCl_2$, 2.5 mM $CaCl_2$, and 11 mM glucose. Whole-cell recordings were performed with patch pipettes (1 to 5 megohms) containing 10 mM Hepes (pH 7.1), 140 mM KCl, 2 mM $MgCl_2$, 1 mM $CaCl_2$, 11 mM EGTA, and 2 mM adenosine triphosphate. Drugs and normal Krebs were applied to the HEK293 cells and neurons with a rapid perfusion system consisting of a multibarreled electrode made from Quad glass tubing (Clarks Electromedical, Reading, UK) that was positioned within 50 to 100 μm of the cell. Solution exchange with this perfusion system occurred in ~4 ms. The HEK293 cells were used for recording 48 hours after transfection and had resting potentials of −30 to −60 mV. Transfection with wild-type or mutant cDNAs was performed on different cultures of HEK293 cells derived from the same parent colony. As a result of the variation in transfection efficiency, the amplitudes of GABA currents recorded with both the wild-type and the mutant GABA receptors in the absence of cAMP or PKA were quite variable between cells. Comparison of the GABA currents recorded from 29 to 45 cells transfected with either the wild-type or mutant cDNAs for the $\alpha_1\beta_1$ or $\alpha_1\beta_1\gamma_2$ combinations in the absence of cAMP, PKA, or Cα did not reveal any significant differences between their response amplitudes or kinetics. Voltage-clamp currents were recorded with a List (Darmstadt, Germany) EPC7 amplifier, displayed on a Brush-Gould (London) ink-jet pen recorder (2400S), and stored on a Racal (Southampton, UK) store 4DS tape recorder (direct current to 5 kHz). Neurons were cultured from rat superior cervical ganglia of embryonic day 21 (E21) animals as described (*16*). Neurons were used 2 to 4 days after dissociation and had membrane potentials of −50 to −70 mV and action potential amplitudes of 80 to 95 mV. Recordings were made from neurons as described above.
14. T. A. Verdoorn, A. Draguhn, S. Ymer, P. H. Seeburg, B. Sakmann, *Neuron* **4**, 919 (1990).
15. T. G. Smart, S. J. Moss, X. Xie, R. L. Huganir, *Brit. J. Pharmacol.* **103**, 1837 (1991).
16. T. G. Smart, *J. Physiol. (London)* **447**, 587 (1992).
17. A. Draguhn, T. A. Verdoorn, M. Ewert, P. H. Seeburg, B. Sakmann, *Neuron* **5**, 781 (1990).
18. N. J. Leidenheimer, M. D. Browning, R. A. Harris, *Trends Pharmacol. Sci.* **12**, 84 (1991).
19. M. D. Browning, M. Bureau, E. M. Dudek, R. W. Olsen, *Proc. Natl. Acad. Sci. U.S.A.* **87**, 1315 (1990).
20. E. F. Kirkness, C. F. Bovenkerk, T. Ueda, A. J. Turner, *Biochem. J.* **259**, 613 (1989).
21. N. J. Leidenheimer *et al.*, *J. Neurochem.* **57**, 722 (1991).
22. N. M. Porter, R. E. Twyman, M. D. Uhler, R. L. MacDonald, *Neuron* **5**, 789 (1990).
23. E. Sigel and R. Bauer, *Proc. Natl. Acad. Sci. U.S.A.* **85**, 6192 (1988).
24. F. M. Sessler *et al.*, *Brain Res.* **499**, 27 (1989).
25. M. K. Ticku and A. K. Mehta, *Mol. Pharmacol.* **38**, 719 (1990).
26. R. L. Huganir, A. H. Delcour, P. Greengard, G. P. Hess, *Nature* **321**, 774 (1986); J. F. Hopfield, D. W. Tank, P. Greengard, R. L. Huganir, *ibid.* **336**, 677 (1988).
27. P. Kofuji, J. B. Wang, S. J. Moss, R. L. Huganir, D. R. Burt, *J. Neurochem.* **56**, 713 (1991).
28. J. B. Wang *et al.*, *J. Mol. Neurosci.*, in press.
29. T. A. Kunkel, J. D. Roberts, D. L. Zabour, *Methods Enzymol.* **154**, 367 (1987).
30. R. L. Huganir, K. Miles, P. Greengard, *Proc. Natl. Acad. Sci. U.S.A.* **81**, 6968 (1984).
31. Supported by the Howard Hughes Medical Institute, the Medical Research Council (United Kingdom), and the Wellcome Trust. We thank M. D. Uhler (University of Michigan) for the cDNA clones of the catalytic subunit of the cAMP-dependent protein kinase and L. Raymond for critical review of the manuscript.

19 March 1992; accepted 11 June 1992

Neuronal Domains in Developing Neocortex

Rafael Yuste,* Alejandro Peinado, Lawrence C. Katz

The mammalian neocortex consists of a mosaic of columnar units whose development is poorly understood. Optical recordings of brain slices labeled with the fluorescent calcium indicator fura-2 revealed that the neonatal rat cortex was partitioned into distinct domains of spontaneously coactive neurons. In tangential slices, these domains were 50 to 120 micrometers in diameter; in coronal slices they spanned several cortical layers and resembled columns found in the adult cortex. In developing somatosensory cortex, domains were smaller than, and distinct from, the barrels, which represent sensory input from a single vibrissa. The neurons within each domain were coupled by gap junctions. Thus, nonsynaptic communication during cortical development defines discrete multicellular patterns that could presage adult functional architecture.

In mammalian neocortex, local circuits are preferentially organized in a radial direction, forming a modular architecture of columnar units (*1*). At least two possible developmental mechanisms, not mutually exclusive, could generate cortical columns. By analogy with the formation of ocular dominance stripes or clustered horizontal connections (*2*), columns could arise by activity-dependent formation, selection, or enhancement of connections in the vertical dimension. A different explanation—the "radial unit" hypothesis—has been formulated by Rakic (*3*). According to this theory, polyclones of developing neurons migrate to the cortex along radial glial fibers and, based on their migratory history, form radial units, which subsequently differentiate into adult columns. Both hypotheses require the presence of some type of mechanism, early in cortical development, to inform neurons that they are members of a distinct radial group. By visualizing patterns of multicellular activity, we have revealed the existence of one such possible mechanism.

To study the behavior of cortical networks as local microcircuits emerge, we used optical recordings with the Ca^{2+}-sensitive indicator fura-2 (*4*) in slices of developing rat cortex. Because neuronal activity is associated with presynaptic and postsynaptic Ca^{2+} influx (*5*), imaging of neuronal populations labeled with Ca^{2+}-sensitive indicators offers a sensitive method for optical recording of both suprathreshold and subthreshold events. Fura-2 can be used in slices of developing neocortex to reveal transmitter-induced Ca^{2+} changes in neurons (*6*); we have applied this approach to visualize multicellular patterns of spontaneous activity in these slices.

Optical recordings (*7*) were carried out in 12 coronal (across layers) and 12 tangential (parallel to the layers) slices obtained from somatosensory, visual, and frontal cortices of rats during postnatal days (PND) 0

Table 1. Total number of domains recorded and the instances of recurrences in 24 tangential (t) and coronal (c) cortical slices from PND 0 to 7 rats. PND 0 is the day of birth.

Age (PND), orientation	Number of domains	Recording time (s)	Number of recurrences
4, c	61	9596	16
5, c	38	8018	2
5, c	37	8008	6
4, c	37	5604	5
4, t	35	5876	3
5, t	35	7928	9
5, c	35	7216	3
3, c	34	10624	3
5, t	33	1200	3
4, c	27	4808	8
5, t	18	4800	1
4, t	16	1220	1
6, c	16	6192	0
4, c	15	3504	0
0, c	15	1396	0
5, t	13	8052	0
6, t	11	2812	1
6, t	8	2808	3
1, c	8	800	0
5, t	7	4472	0
6, t	5	4408	0
5, t	5	2576	0
1, c	5	4088	0
7, t	3	2300	0

Department of Neurobiology, Box 3209, Duke University Medical Center, Durham, NC 27710.

*To whom correspondence should be addressed.